Novel Andreev reflection and differential conductance of a ferromagnet/ferromagnet/superconductor junction on graphene

2009 J. Phys.: Condens. Matter 21 095302

(http://iopscience.iop.org/0953-8984/21/9/095302)

IOP PUBLISHING JOURNAL OF PHYSICS: CONDENSED MATTER

J. Phys.: Condens. Matter **21** (2009) 095302 (6pp) doi:10.1088/0953-8984/21/9/095302

Novel Andreev reflection and differential conductance of a ferromagnet/ferromagnet/superconductor junction on graphene

Zhi-Yong Zhang

Department of Physics, Nanjing University, Nanjing 210093, People's Republic of China

Received 15 August 2008, in final form 20 December 2008
Published 4 February 2009
Online at stacks.iop.org/JPhysCM/21/095302

Abstract

Via numerical calculation of the spin-dependent Dirac–Bogoliubov–de Gennes equation, the differential conductance is obtained for a ferromagnet/ferromagnet/superconductor (F/F/S) junction on graphene where the two F layers are undoped. If the two F layers have noncollinear magnetizations, the spin-flipped scattering at the F/F interface leads to the novel Andreev reflection (AR), in which the spin directions of an incident electron and the reflected hole are opposite to each other. When the exchange energy is larger than the superconducting gap, this novel AR manifests itself as sub-gap differential conductance peaks because of the formation of spin-flipped Andreev bound states in the intermediate F layer, whereas for the parallel and anti-parallel configurations no such peaks can be found. In the transitional regime with the exchange energy close to the gap, for noncollinear configurations, the round-trip path supporting the formation of those bound states is broken and a differential conductance dip can be found near the point where the external bias equals the exchange energy.

(Some figures in this article are in colour only in the electronic version)

1. Introduction

Recent fabrication of graphene [1], a monatomic layer of graphite with a honeycomb lattice structure, provides the opportunity for employing its unusual low-energy electronic properties to design novel micro-electronic devices. Undoped graphene has six discrete Fermi points, corresponding to the corners of the hexagonal Brillouin zone, out of which only two are inequivalent. In the vicinity of these two valleys, the excitation spectrum obeys a Dirac-like Hamiltonian [2], which yields a linear energy dispersion instead of a parabolic one (cf figure 1). The electronic and hole states are interconnected, and chirality, the projection of pseudo-spin on the direction of motion, is conserved in the tunneling process [3]. It is of theoretical interest and of technological importance to investigate how such unusual low-energy electronic structures affect the transport properties under the influence of long-range correlations, such as superconductivity and magnetism [4–9].

The state-of-the-art fabrication technology can introduce these types of correlations in graphene via the proximity effect. A measurable supercurrent has been observed between regions of graphene under the influence of proximity-induced superconductivity [10, 11]. It has been shown that ferromagnetic correlation can be induced in graphene by means of an external electrical field [12, 13]. Other suggestions are proposed to achieve magnetism in graphene by exploiting a

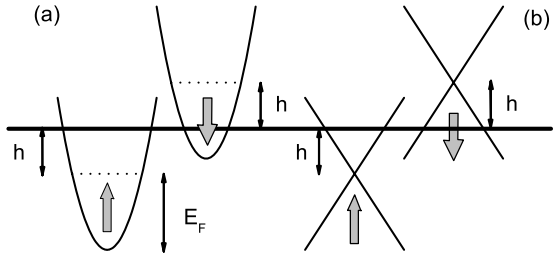

Figure 1. Energy spectra of (a) usual F metal with $E_F \neq 0$ and (b) undoped F graphene with $E_F = 0$. The exchange field is assumed to be parallel to the z axis, and $\Uparrow$ and $\Downarrow$ denote the spin-up and spin-down electrons, respectively.

magnetic gate in contact with a graphene layer [8, 14]. The proximity layer can be made up of a magnetic insulator [15], such as EuO, or a multiferroic material, e.g. $BiFeO_3$ [16], so that the magnetization in the proximity layer, and consequently the exchange field in the graphene, can be tuned by an external magnetic field in the former case and an electric field in the later. Long electronic mean free paths [17] and large spin relaxation times [18] of the carbon-based system make graphene an attractive candidate for the observation of near-ballistic spin transport.

Spin-dependent transport through ferromagnet/superconductor (F/S) junctions is an important subject in the field of spintronics, which has recently attracted a lot of attention because of the hope of fabricating novel devices manipulating spin in addition to charge [19–21]. Suppose the superconductor has the s-wave pairing symmetry. When a spin-up electron is incident from the normal side with its energy below the superconducting gap Δ, a Cooper pair is injected into the S side with a spin-up hole reflected, which is known as Andreev reflection (AR) [22]. In this process, spin-singlet pairing states are formed near the interface. However, in the usual F/S junctions, due to the spin polarization caused by the exchange field in ferromagnetic metals, (cf figure 1(a), where the spin-down electrons are minority particles) the AR is suppressed [23] and the sub-gap differential conductance is decreased [24–29]. If a two-dimensional electronic gas (2DEG) with the Rashba spin–orbit coupling is inserted between the F and S parts, the spin precession in the 2DEG can lead to the so-called novel AR, in which the incident electron and the reflected hole have opposite spin directions. As a result, spin-triplet pairing states are formed near the interface and the sub-gap differential conductance is enhanced [30].

The idea of novel AR was first introduced by Niu and Xing in their studies of the spin-triplet pairing states in F/F/d-wave superconductor heterojunctions with noncollinear magnetizations [31]. However, in the usual F/F/S junctions with half-metallic F layers, the exponential damping in the intermediate F layer prevents the Andreev-reflected spin-up hole to be spin-flipped at the F/F interface since the minority spin conduction band has its bottom. In graphene, the conduction band is interconnected with the valence band, (cf figure 1(b)) and the 'minority' spin propagation in the intermediate F layer is not exponentially damped [32, 33]. For F/F/S junctions on graphene with noncollinear magnetizations, the spin-flipped scattering at the F/F interface can lead to the novel AR even if the exchange energy h is much larger than the Fermi energy E_F. In the present work, we investigate how the novel AR influences the differential conductance through an F/F/S junction on graphene with two undoped F layers.

For this purpose, the differential conductance through the F/F/S junction is obtained via numerical calculation of the spin-dependent Dirac–Bogoliubov–de Gennes (DBdG) equation [4, 5, 9, 32, 33]. Here, the S layer is assumed to have the s-wave pairing symmetry. If the two F layers have noncollinear magnetizations, the spin-flipped scattering at the F/F interface leads to the novel AR as expected. In the situation with $h \gg \Delta$, this novel AR manifests itself as sub-gap differential conductance peaks because of the formation of spin-flipped Andreev bound states in the intermediate F layer, whereas for the parallel and anti-parallel configurations no sub-gap peak can be found. In the transitional regime with $h \sim \Delta$, for noncollinear magnetizations, the round-trip path supporting the formation of those bound states is broken and a differential conductance dip can be found near the point $E = h$.

The organization of this paper is as follows. In section 2, the theoretical model is presented. In section 3, the numerical results are illustrated and discussed. A brief summary is given in section 4.

2. Model and formulae

In the present paper, we calculate the differential conductance through an F/F/S junction formed on a graphene sheet, which is assumed to be the xy plane. The F/F and F/S interfaces are located at $x = -L$ and $x = 0$, respectively, and the translational invariance is kept in the y direction. In the left F layer, the magnetization is along the z axis, whereas it points to the direction $(0, \sin\theta, \cos\theta)$ in the middle F layer. The S layer is assumed to have the s-wave pairing symmetry. Neglecting the self-consistency of the spatial distribution of the pair potential in the S layer, we take the pair potential as $\Delta(x) = \Delta\Theta(x)$ with $\Theta(x)$ the Heaviside function. The electrostatic potentials in different regions can be adjusted independently by separate gate voltages or by different doping levels. For simplicity, the potentials are assumed to be the same in the two F layers, which have a potential difference U with the S layer. Although in the present work, what we are interested in is the F/F/S junction with two undoped F layers where $E_F = 0$, for the use of subsequent works, E_F is retained in the formulae. To deal with superconductivity via the mean-field approximation, the restriction $\Delta \ll E_F + U$ should be satisfied.

The low-energy electronic and hole excitations in the F/F/S junction can be described by the following spin-dependent DBdG equation [4–6, 9, 32–34]:

$$\begin{pmatrix} \hat{H}_\tau - \hat{\vec{s}}\cdot\vec{h}(x) + V(x) - E_F & \Delta(x) \\ \Delta(x) & E_F - V(x) - \hat{H}_\tau - \hat{\vec{s}}\cdot\vec{h}(x) \end{pmatrix} \Psi_\tau = E\Psi_\tau \quad (1)$$

with $\tau = K, K'$, the valley index. In the valley $K(K')$, $\hat{H}_{K(K')} = -i\hbar v_F(\hat{\sigma}_x\partial_x + (-)\hat{\sigma}_y\partial_y)$ with $v_F \approx 10^6$ m s^{-1}. Here, $\hat{\vec{s}}$ and $\hat{\vec{\sigma}}$ are 2×2 Pauli matrices operating in the spin and sublattice subspaces, respectively. $V(x) = -U\Theta(x)$ and $\vec{h}(x) = h\Theta(-x)(0, \sin\theta(x), \cos\theta(x))$ with $\theta(x) = 0$ for $x < -L$ and θ for $-L < x < 0$. Via time-reversal transformation, the electron-like and hole-like parts of the spinor Ψ_τ are related to each other. Taking into account the spin degree of freedom, the time-reversal operator is $\mathcal{T} = \hat{\tau}_x \otimes (-i\hat{s}_y) \otimes \hat{\sigma}_z\mathcal{C}$ with $\mathcal{C}$ the operator of complex conjugate [35]. As a result, $\Psi_K = (\Phi_{K\uparrow A}, \Phi_{K\uparrow B}, \Phi_{K\downarrow A}, \Phi_{K\downarrow B}, -\Phi^*_{K'\downarrow A}, \Phi^*_{K'\downarrow B}, \Phi^*_{K'\uparrow A}, -\Phi^*_{K'\uparrow B})^T$. In a similar way, $\Psi_{K'}$ can be obtained. Due to the valley degeneracy, only $\hat{H}_K$ is considered in our calculation and the subscript K is omitted.

When an electron with energy E is incident from the left F layer, the wavenumber in the transverse direction, k_y, is

conserved in the tunneling process. The states of electronic and hole excitations in this layer are: $\phi^{\rm e}_{\uparrow}(\alpha^{\rm e}_{\uparrow}) = \frac{1}{\sqrt{2}}(1,0)^{\rm T} \otimes (1,0)^{\rm T} \otimes (1, {\rm e}^{{\rm i}\alpha^{\rm e}_{\uparrow}})^{\rm T}{\rm e}^{{\rm i}k^{\rm e}_{\uparrow}\cos\alpha^{\rm e}_{\uparrow}x}$, $\phi^{\rm e}_{\downarrow}(\alpha^{\rm e}_{\downarrow}) = \frac{1}{\sqrt{2}}(1,0)^{\rm T} \otimes (0,1)^{\rm T} \otimes (1, {\rm e}^{{\rm i}\alpha^{\rm e}_{\downarrow}})^{\rm T}{\rm e}^{{\rm i}k^{\rm e}_{\downarrow}\cos\alpha^{\rm e}_{\downarrow}x}$, $\phi^{\rm h}_{\uparrow}(\alpha^{\rm h}_{\uparrow}) = \frac{1}{\sqrt{2}}(0,1)^{\rm T} \otimes (1,0)^{\rm T} \otimes (1, -{\rm e}^{{\rm i}\alpha^{\rm h}_{\uparrow}})^{\rm T}{\rm e}^{{\rm i}k^{\rm h}_{\uparrow}\cos\alpha^{\rm h}_{\uparrow}x}$ and $\phi^{\rm h}_{\downarrow}(\alpha^{\rm h}_{\downarrow}) = \frac{1}{\sqrt{2}}(0,1)^{\rm T} \otimes (0,1)^{\rm T} \otimes (1, -{\rm e}^{{\rm i}\alpha^{\rm h}_{\downarrow}})^{\rm T}{\rm e}^{{\rm i}k^{\rm h}_{\downarrow}\cos\alpha^{\rm h}_{\downarrow}x}$. Here, $k^{\tau}_{\uparrow} = (E \pm E_{\rm F} + h)/(\hbar v_{\rm F})k^{\tau}_{\downarrow} = (E \pm E_{\rm F} - h)/(\hbar v_{\rm F})$ with the signs + and − corresponding to $\tau = {\rm e}$ and h, respectively, and $\alpha^{\tau}_{s} = \sin^{-1}(k_y/k^{\tau}_{s})$. In the above states, a common factor ${\rm e}^{{\rm i}k_y y}$ is omitted for clarity. With the incident electron having spin s, the total wavefunction in this layer can be written as

$$\Psi_s = \phi^{\rm e}_{s}(\alpha^{\rm e}_{s}) + \sum_{s'}(r_{s's}\phi^{\rm e}_{s'}(\tilde{\alpha}^{\rm e}_{s'}) + r^{A}_{s's}\phi^{\rm h}_{s'}(\tilde{\alpha}^{\rm h}_{s'})) \qquad (2)$$

with $\tilde{\alpha}^{\tau}_{s'} = (\pi - |\alpha^{\tau}_{s'}|)\alpha^{\tau}_{s'}/|\alpha^{\tau}_{s'}|$.

In the middle F layer, with the magnetization rotating an angle θ around the x axis compared to that in the left F layer, the electron and hole spinors rotate in the spin subspace and the corresponding sub-spinors change from $(1,0)^{\rm T}$ and $(0,1)^{\rm T}$ to $(\cos\frac{\theta}{2}, {\rm i}\sin\frac{\theta}{2})^{\rm T}$ and $({\rm i}\sin\frac{\theta}{2}, \cos\frac{\theta}{2})^{\rm T}$, respectively, whereas the components in the Nambu and sublattice spaces remain unchanged. With these new spinors written as φ^{τ}_{s}, the total wavefunction in this region is

$$\Psi_s = \sum_{\tau,s'}(a^{\tau}_{s's}\varphi^{\tau}_{s'}(\alpha^{\tau}_{s'}) + b^{\tau}_{s's}\varphi^{\tau}_{s'}(\tilde{\alpha}^{\tau}_{s'})). \qquad (3)$$

In the S layer, the electron- and hole-like excitations are given as $\psi^{\rm e}_{\uparrow}(\beta^{\rm e}) = \frac{1}{\sqrt{2}}(u,v)^{\rm T} \otimes (1,0)^{\rm T} \otimes (1, {\rm e}^{{\rm i}\beta^{\rm e}})^{\rm T}{\rm e}^{{\rm i}p^{\rm e}\cos\beta^{\rm e}x}$, $\psi^{\rm e}_{\downarrow}(\beta^{\rm e}) = \frac{1}{\sqrt{2}}(u,v)^{\rm T} \otimes (0,1)^{\rm T} \otimes (1, {\rm e}^{{\rm i}\beta^{\rm e}})^{\rm T}{\rm e}^{{\rm i}p^{\rm e}\cos\beta^{\rm e}x}$, $\psi^{\rm h}_{\uparrow}(\beta^{\rm h}) = \frac{1}{\sqrt{2}}(v,u)^{\rm T} \otimes (1,0)^{\rm T} \otimes (1, {\rm e}^{{\rm i}\beta^{\rm h}})^{\rm T}{\rm e}^{{\rm i}p^{\rm h}\cos\beta^{\rm h}x}$ and $\psi^{\rm h}_{\downarrow}(\beta^{\rm h}) = \frac{1}{\sqrt{2}}(v,u)^{\rm T} \otimes (0,1)^{\rm T} \otimes (1, {\rm e}^{{\rm i}\beta^{\rm h}})^{\rm T}{\rm e}^{{\rm i}p^{\rm h}\cos\beta^{\rm h}x}$. Here, $p^{\tau} = (\pm\sqrt{E^2 - \Delta^2} + E_{\rm F} + U)/(\hbar v_{\rm F})$ and $\beta^{\tau} = \sin^{-1}(k_y/p^{\tau})$. The superconductor coherent factors u and v are $u = \sqrt{[1 + E^{-1}(E^2 - \Delta^2)^{1/2}]/2}$ and $v = \sqrt{[1 - E^{-1}(E^2 - \Delta^2)^{1/2}]/2}$. Then in the S layer, the total wavefunction is

$$\Psi_s = \sum_{s'}\left(t^{\rm e}_{s's}\psi^{\rm e}_{s'}(\beta^{\rm e}) + t^{\rm h}_{s's}\psi^{\rm h}_{s'}(\pi - \beta^{\rm h})\right). \qquad (4)$$

From the boundary condition, i.e. the continuity of the wavefunction Ψ_s at the interfaces, all of the superposition coefficients in the above three equations can be obtained. For the F/F/S junction, which is W in width, k_y can only take a series of quantized values. In the limit $W \to \infty$, N_s, the number of discrete k_y is much larger than unity with $N_s \gg 1$, and the differential conductance can be obtained, instead from a summation of contributions of quantized transverse modes, from an integration over k_y. Then the zero-temperature differential conductance of the F/F/S junction can be written as [4, 5, 9, 14, 36]

$$G(E) = \sum_{s=\uparrow,\downarrow}\frac{1}{|k^{\rm e}_{s}|}\int_0^{|k^{\rm e}_{s}|}{\rm d}k_y\, G_s(E,k_y), \qquad (5)$$

where

$$G_s(E,k_y) = \frac{N_s}{N_\uparrow + N_\downarrow} \times \sum_{s'}\left(\delta_{s's} - |r_{s's}|^2\frac{\cos\alpha^{\rm e}_{s'}}{\cos\alpha^{\rm e}_{s}} + |r^{A}_{s's}|^2\frac{\cos\alpha^{\rm h}_{s'}}{\cos\alpha^{\rm e}_{s}}\right). \qquad (6)$$

Here, $N_s = |k^{\rm e}_{s}|W/\pi$ is the number of allowed k_y when a spin s electron with energy E is incident into the junction [37]. In the above two equations, the differential conductance is normalized with $\frac{2{\rm e}^2}{h}(N_\uparrow + N_\downarrow)$ and the factor 2 is the valley degeneracy.

In the present work, what we are interested in is the F/F/S junction with two undoped F layers. In this junction, $E_{\rm F} = 0$, $k^{\rm e}_{\uparrow} = k^{\rm h}_{\uparrow} = E + h$ and $k^{\rm e}_{\downarrow} = k^{\rm h}_{\downarrow} = E - h$. At $E = h$, $N_\downarrow = 0$, but the condition $N_\downarrow \gg 1$ is satisfied at all of the other points for a large W. If $k_y > |E - h|$, the novel AR with a spin ↑ electron converted to a spin ↓ hole is forbidden, but the other novel AR with a spin ↓ electron converted to a spin ↑ hole and the two types of usual AR are still permitted in this F/F/S junction.

3. Results and discussion

Before turning our attention to the numerical data, we first analyze the tunneling process through this F/F/S junction qualitatively. When $\theta = 0$ or π, no spin flip can take place at the F/F interface and the 8×8 spin-dependent DBdG Hamiltonian can be decomposed into two independent 4×4 ones for the spin-up and spin-down spinors, where the exchange energy can be simply treated as an effective electrostatic potential [9, 32, 33]. In these two configurations, $r_{\downarrow\uparrow} = r_{\uparrow\downarrow} = r^{A}_{\downarrow\uparrow} = r^{A}_{\uparrow\downarrow} = 0$. Only the usual AR can assist the sub-gap tunneling and spin-singlet pairing states are formed near the F/S interface. If the magnetizations of the two F layers are noncollinear, the spin-flipped scattering can take place at the F/F interface. With a spin-up electron incident into the junction, not only a spin-up hole but also a spin-down hole can be reflected. This is the so-called novel AR [30, 31] and spin-triplet pairing states are formed near the F/S interface. The novel AR shows entirely different characteristics in the situations with $h \gg \Delta$ and with $h \ll \Delta$. In the former, the low-energy spectrum of undoped graphene with exchange energy h (cf figure 1(b)) shows that, at the F/S interface, the AR is specular [4]. That is, in the process of electron–hole conversion, the direction of transverse movement is kept. At the F/F interface, although the spin-conserved reflection is specular, the spin-flipped reflection is a retro-reflection, i.e. the direction of transverse movement is reversed. The specular AR at the F/S interface and the spin-flipped retro-reflection at the F/F interface constitute a round-trip path, which leads to the formation of spin-flipped Andreev bound states in the intermediate F layer. When $h \ll \Delta$, the F/F/S junction reduces to the corresponding spin-degenerate system which has been studied in [4]. When $h \sim \Delta$, the spin-flipped Andreev bound states can still be formed if $E < h$. However, if $E > h$, although the electron–hole conversion still takes place via specular Andreev reflection, the reflection at the F/F interface is always specular no matter whether the spin is flipped or

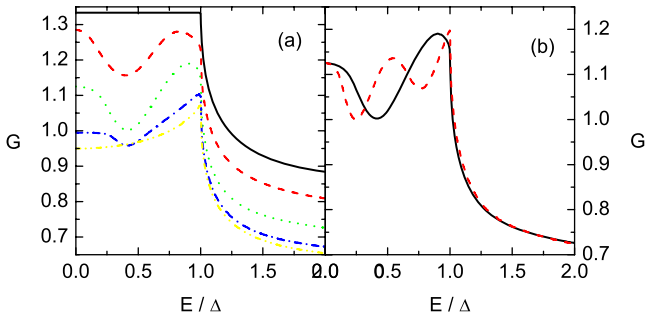

Figure 2. (a) G–E curves with $\Delta L/(\hbar v_{\rm F}) = 1$ for $\theta = 0$ (black solid), $\pi/4$ (red dashed), $\pi/2$ (green dotted), $3\pi/4$ (blue dashed–dotted) and π (yellow dash–dot–dotted). (b) G–E curves for $\theta = \pi/2$ with $\Delta L/\hbar v_{\rm F} = 1$ (black solid) and $\Delta L/(\hbar v_{\rm F}) = 2$ (red dashed). The other parameters are $h = U = 100\Delta$ and $E_{\rm F} = 0$.

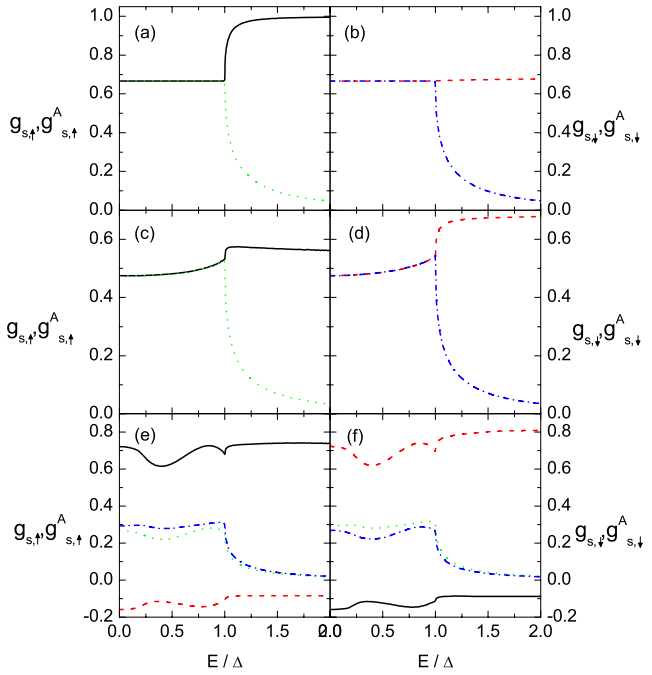

Figure 3. Variations of $g_{\uparrow s}$ (black solid), $g_{\downarrow s}$ (red dashed), $g^A_{\uparrow s}$ (green dotted) and $g^A_{\downarrow s}$ (blue dashed–dotted) with E for $\theta = 0$ ((a) and (b)), π ((c) and (d)) and $\pi/2$ ((e) and (f)). In the left column, $s = \uparrow$ and in the right $s = \downarrow$. The other parameters are $\Delta L/(\hbar v_{\rm F}) = 1$, $h = U = 100\Delta$ and $E_{\rm F} = 0$.

conserved. This breaks the round-trip path and consequently the spin-flipped Andreev bound states [38].

Now, we turn our attention to the numerical data and first consider the situation with $h \gg \Delta$. In this situation, it is assumed that $h = U = 100\Delta$. The corresponding G–E curves with θ increased from 0 to π in steps of $\pi/4$ are presented in figure 2(a). For $\theta = 0$, the F/F/S junction can be looked at as an F/S junction. In this configuration, the sub-gap differential conductance takes a constant value $4/3$. This is entirely different from the usual half-metallic F/S junctions where the AR is suppressed by the spin polarization. The reason has been analyzed in the above paragraph. For $\theta = \pi$, the magnetizations of the two F layers are in an anti-parallel configuration and the exchange field simply causes a mismatch of effective electrostatic potential between the two F layers. As a result, the differential conductance is depressed compared with the parallel configuration and a peak is located at the gap edge. With the exchange energy h enhanced, the sub-gap G is reduced for both the parallel and antiparallel configurations, but a sub-gap peak can never be found.

Compared with the parallel and anti-parallel configurations, the most remarkable feature of the F/F/S junctions with noncollinear magnetizations is the appearance of differential conductance peaks in the gap. This is a direct manifestation of the formation of spin-flipped Andreev bound states in the intermediate F layer. The peak–valley contrast is related with θ. When $\theta = \pi/2$, the largest probability for spin-flipped reflection to take place leads to the strongest peak–valley contrast. With the magnetizations close to the parallel and antiparallel configurations, the contrast becomes weak. Varying the exchange energy h cannot change the number of sub-gap peaks. For the F/F/S junction studied here with $\Delta L/(\hbar v_{\rm F}) = 1$, two sub-gap peaks can be found, one of which is located at the gap center. Since the sub-gap differential conductance peaks are caused by the formation of spin-flipped Andreev bound states in the intermediate F layer, if the length of the round-trip path is increased, more peaks should appear. In figure 2(b), the G–E curve at $\theta = \pi/2$ is plotted for $\Delta L/(\hbar v_{\rm F}) = 2$. In this circumstance, three sub-gap peaks are found, one of which is still located at the gap center, whereas with $\theta = 0$ or π, the sub-gap differential conductance is almost unchanged with L. The contrast between the configurations with collinear and noncollinear magnetizations proves that spin-flipped Andreev bound states are formed in the latter.

To further verify the existence of novel AR in the transport through the F/F/S junction on graphene, the variation of $g_{s's}$ and $g^A_{s's}$ with E is plotted in figure 3 for parallel and antiparallel configurations and for $\theta = \pi/2$. Here, $g_{s's} = \frac{1}{|k^{\rm e}_s|}\int_0^{|k^{\rm e}_s|} {\rm d}k_y\,(\delta_{s's} - |r_{s's}|^2 \frac{\cos\alpha^{\rm e}_{s'}}{\cos\alpha^{\rm e}_s})$ and $g^A_{s's} = \frac{1}{|k^{\rm e}_s|}\int_0^{|k^{\rm e}_s|} {\rm d}k_y\,|r^A_{s's}|^2 \frac{\cos\alpha^{\rm h}_{s'}}{\cos\alpha^{\rm e}_s}$. As expected, only with noncollinear magnetizations can spin-flipped scattering take place, which results in the novel AR with nonzero $g^A_{\downarrow\uparrow}$ and $g^A_{\uparrow\downarrow}$. With collinear magnetizations, only spin-conserved scattering and consequently the usual AR take place. For the parallel configuration, $g_{\uparrow\uparrow} = g_{\downarrow\downarrow}$ and $g^A_{\uparrow\uparrow} = g^A_{\downarrow\downarrow}$ in the gap since the low-energy spectra of spin-up (-down) electrons and spin-up (-down) holes are identical when $E_{\rm F} = 0$. For the anti-parallel configuration, these two equations hold only at $E = 0$, and with E increased they are broken, but this breaking is weak since the difference between $E + h$ and $|E - h|$ is very small for $h \gg \Delta$. A similar phenomenon can also be found between $g_{\downarrow\uparrow}$ and $g_{\uparrow\downarrow}$ and between $g^A_{\downarrow\uparrow}$ and $g^A_{\uparrow\downarrow}$ when noncollinear magnetizations are taken. Although all of the above results are obtained at $E_{\rm F} = 0$, the spin-flipped Andreev bound states can be formed for $E_{\rm F} \neq 0$ only if the two conditions $h + E_{\rm F} \gg \Delta$ and $h - E_{\rm F} \gg \Delta$ are satisfied. With h decreased, similar results can be found until $h \sim 10\Delta$.

Next, we consider the situation with $h \sim \Delta$. In figures 4(a) and (b), the G–E curves are presented for $\theta = \pi/2$ and π, respectively, which correspond to the noncollinear

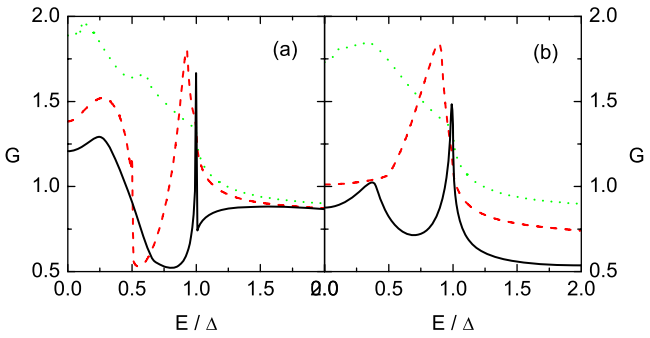

Figure 4. G–E curves for $\theta = \pi/2$ (a) and π (b) with $h = \Delta$ (black solid), $\Delta/2$ (red dashed) and $\Delta/10$ (green dotted). The other parameters are the same as in figure 3.

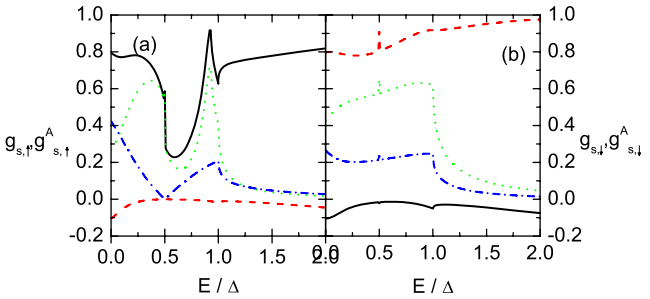

Figure 5. The same as figure 3 for $\theta = \pi/2$ with $h = \Delta/2$.

and antiparallel configurations. Here, the results for $\theta = 0$ are not given because the differential conductance for the parallel configuration at $h = 10\Delta$ already shows the characteristics of the corresponding spin-degenerate system. For the noncollinear configuration, at the point $E = h$, the novel AR with a spin $\uparrow$ electron converted to a spin $\downarrow$ hole is forbidden, and only the usual AR from spin $\uparrow$ electrons to spin $\uparrow$ holes contributes to $G_\uparrow$. Meanwhile, near this point, $|k^{\mathrm{e}}_\downarrow| \ll |k^{\mathrm{e}}_\uparrow|$ and the contribution to G mainly comes from $G_\uparrow$. As a result, a large dip can be found near this point and the dip cannot reach to zero [4]. The position of this dip cannot be moved by the variation of L, but with $h \ll \Delta$, for example with $h = \Delta/10$, the dip disappears. For the antiparallel configuration, a dip can also be found when $h = \Delta$, but this sub-gap dip comes neither from the formation of spin-flipped Andreev bound states nor from the forbidding of some type of novel AR at a special point, but from the complicated effect of multiscattering between the F/F and F/S interfaces, and its position varies with L. For $\Delta L/(\hbar v_{\mathrm{F}}) = 1$, this dip already disappears at $h = \Delta/2$. As shown from the differential conductance in figure 4, with h decreased from Δ to $\Delta/10$, the F/F/S junction gradually reduces to the corresponding spin-degenerate system [4]. To further clarify the underlying physics in this situation, the $g_{s's}$–E and $g^A_{s's}$–E curves with $h = \Delta/2$ are plotted in figure 5 for $\theta = \pi/2$. At $E = h = \Delta/2$, $g_{\downarrow\uparrow}$ and $g^A_{\downarrow\uparrow}$ are zero since $k^{\mathrm{e}}_\downarrow = k^{\mathrm{h}}_\downarrow = 0$. Because of the same reason, a small sharp peak or dip can be found at this point in the $g_{s\downarrow}$–E and $g^A_{s\downarrow}$–E curves.

The recent experimental observation of electron–hole puddles in graphene [39] suggests that such charge inhomogeneities play an important role in the transport characteristics of graphene close to the Dirac point. In the F/F/S junction with $h \gg \Delta$, the general phenomena of novel AR and formation of spin-flipped Andreev bound states should pertain although the wavefunctions are no longer plane waves.

In the above discussion, electrons are incident from the left F layer and into the S layer, and our attention is focused on the spin-flipped Andreev bound states. If, on the other hand, three terminals are attached to the two F and the S layers, respectively, and electrons are incident from the left F layer, the Andreev-reflected holes can leave the junction from the terminal attached to the middle F layer. In this situation, the electrons dragged into the middle F layer have different spin directions from those incident into the left F layer. This is the so-called nonlocal or crossed Andreev reflection (CAR), which is usually found in F/S/F junctions with half-metallic F layers. The special dispersion relation of graphene in the vicinity of the two valleys allows the reflection-type CAR. The study of characteristics of this reflection-type CAR and its application [7] is an interesting topic in future work.

In the present paper, only the s-wave pairing symmetry is considered. As we know, the spin-singlet Cooper pairs also admit the d-wave pairing symmetry. In this situation, the existence of line nodes that cross the Fermi surface in the gap considerably affects the properties of sub-gap differential conductance, but the mechanism leading to the spin-flipped Andreev bound states still plays an important role. If the proximity layer on the S side has p-wave pairing symmetry, the spin-triplet pairing states are induced in the S layer and the basic physical picture is entirely changed. The study of Andreev reflection and differential conductance under these unconventional pairing symmetries is another interesting topic in future work.

4. Summary

In summary, via numerical calculation of the spin-dependent DBdG equation [4–6, 9, 32, 33], the differential conductance is obtained for an F/F/S junction on graphene with the two undoped F layers. If the two F layers have noncollinear magnetizations, the spin-flipped scattering at the F/F interface leads to the novel AR, in which the incident electron and the reflected hole have opposite spin directions. In the situation with $h \gg \Delta$, this novel AR manifests itself as sub-gap differential conductance peaks because of the formation of spin-flipped Andreev bound states in the intermediate F layer, whereas for the parallel and anti-parallel configurations, no such peak can be found. In the transitional regime with $h \sim \Delta$, the round-trip path supporting the formation of those bound states for noncollinear magnetizations is broken and a differential conductance dip can be found near the point $E = h$, but this dip cannot reach to zero.

Acknowledgment

This work is supported by the National Foundation of Natural Science in China grant No 10874071.

References

[1] Novoselov K S *et al* 2004 *Science* **306** 666
[2] DiVincenzo D P and Mele E J 1984 *Phys. Rev.* B **29** 1685
[3] Katsnelson M I, Novoselov K S and Geim A K 2006 *Nat. Phys.* **2** 620
[4] Beenakker C W J 2006 *Phys. Rev. Lett.* **97** 067007
[5] Bhattacharjee S and Sengupta K 2006 *Phys. Rev. Lett.* **97** 217001
[6] Linder J and Sudbø A 2007 *Phys. Rev. Lett.* **99** 147001
Linder J and Sudbø A 2008 *Phys. Rev.* B **77** 064507
[7] Cayssol J 2008 *Phys. Rev. Lett.* **100** 147001
[8] Semenov Y G, Kim K W and Zavada J M 2007 *Appl. Phys. Lett.* **91** 153105
[9] Linder J, Yokoyama T, Huertas-Hernando D and Sudbø A 2008 *Phys. Rev. Lett.* **100** 187004
[10] Heersche H B *et al* 2007 *Nature* **446** 56
[11] Du X, Skachko I and Andrei E Y 2008 *Phys. Rev.* B **77** 184507
[12] Son Y-W, Cohen M L and Louie S G 2006 *Nature* **444** 347
[13] Kan E-J, Li Z, Yang J and Hou J G 2007 *Appl. Phys. Lett.* **91** 243116
[14] Haugen H, Huertas-Hernando D and Brataas A 2008 *Phys. Rev.* B **77** 115406
[15] Tedrow P M, Tkaczyk J E and Kumar A 1986 *Phys. Rev. Lett.* **56** 1746
[16] Loidl A, von Loehneysen H and Kalvius G M (ed) 2008 *J. Phys.: Condens. Matter* **20** (issue 43)
[17] Geim A K and Novoselov K S 2007 *Nat. Mater.* **6** 183
[18] Min H, Hill J E, Sinitsyn N A, Sahu B R, Kleinman L and MacDonald A H 2006 *Phys. Rev.* B **74** 165310
[19] Prinz G A 1998 *Science* **282** 1660
[20] Awschalom D, Loss D and Samarth N (ed) 2002 *Semiconductor Spintronics and Quantum Computation* (Berlin: Springer)
[21] Zutic I, Fabian J and Das Sarma S 2004 *Rev. Mod. Phys.* **76** 323
[22] Andreev A F 1964 *Zh. Eksp. Teor. Fiz.* **46** 1823
Andreev A F 1964 *Sov. Phys.—JETP* **19** 1228 (Engl. Transl.)
[23] De Jong M J M and Beenakker C W J 1995 *Phys. Rev. Lett.* **74** 1657
[24] Kashiwaya S, Tanaka Y, Yoshida N and Beaslay M R 1999 *Phys. Rev.* B **60** 3572
[25] Zutic I and Valls O T 2000 *Phys. Rev.* B **61** 1555
[26] Stefanakis N 2001 *Phys. Rev.* B **64** 224502
[27] Hirai T, Tanaka Y, Yoshida N, Asano Y, Inoue J and Kashiwaya S 2003 *Phys. Rev.* B **67** 174501
[28] Upadhyay S K, Palanisami A, Louie R N and Buhrman R A 1998 *Phys. Rev. Lett.* **81** 3247
[29] Soulen R J *et al* 1998 *Science* **282** 85
[30] Zhang Z-Y 2008 *Eur. Phys. J.* B **63** 65
[31] Niu Z P and Xing D Y 2007 *Phys. Rev. Lett.* **98** 057005
[32] Asano Y, Yoshida T, Tanaka Y and Golubov A A 2008 *Phys. Rev.* B **78** 014514
[33] Zhang Q, Fu D, Wang B, Zhang R and Xing D Y 2008 *Phys. Rev. Lett.* **101** 047005
[34] De Gennes P G 1966 *Superconductivity of Metals and Alloys* (New York: Benjamin)
[35] Suzuura H and Ando T 2002 *Phys. Rev. Lett.* **89** 266603
[36] Blonder G E, Tinkham M and Klapwijk T M 1982 *Phys. Rev.* B **25** 4515
[37] Tworzydło J, Trauzettel B, Titov M, Rycerz A and Beenakker C W J 2006 *Phys. Rev. Lett.* **96** 246802
[38] Titov M, Ossipov A and Beenakker C W J 2007 *Phys. Rev.* B **75** 045417
[39] Martin J *et al* 2008 *Nat. Phys.* **4** 144